CASE FILE
COPY

WIND-TUNNEL INVESTIGATION OF THE AERODYNAMIC CHARACTERISTICS OF A TWIN-KEEL PARAWING

by George M. Ware

Langley Research Center
Langley Station, Hampton, Va.

WIND-TUNNEL INVESTIGATION OF THE AERODYNAMIC

CHARACTERISTICS OF A TWIN-KEEL PARAWING

By George M. Ware

Langley Research Center
Langley Station, Hampton, Va.

NATIONAL AERONAUTICS AND SPACE ADMINISTRATION

WIND-TUNNEL INVESTIGATION OF THE AERODYNAMIC
CHARACTERISTICS OF A TWIN-KEEL PARAWING

By George M. Ware
Langley Research Center

SUMMARY

An investigation has been conducted in the Langley full-scale tunnel to determine the performance and the static stability and control characteristics of a twin-keel parawing. The model was essentially an all-flexible single-keel parawing configuration with a rectangular panel added to form a center section between the triangular outboard panels. The tests showed that the model had a maximum lift-drag ratio of 3.4. The model was longitudinally stable from the minimum angle of attack attainable before nose collapse up to the stall angle, an angle-of-attack range of about 15°. Changing the length of the aft-keel and wing-tip lines was effective in trimming the model over the entire unstalled angle-of-attack range and resulted in a modulation in lift-drag ratio from 2.2 to 3.4. The model was directionally stable and had positive effective dihedral over the unstalled angle-of-attack range in which the configuration could be trimmed and had longitudinal stability. At angles of attack above the stall, however, the model became directionally unstable and had negative effective dihedral. Differential deflection of the wing tips produced positive rolling moments and negative yawing moments over the test range of angle of attack when the lines were changed in a direction to lower the right wing tip.

INTRODUCTION

The continuing interest in steerable gliding parachutes as a means of space-vehicle recovery and cargo delivery has led to the development of a number of different configurations to meet the demand for such a system. In order to determine the performance, stability and control, and deployment characteristics of this type of decelerator, the National Aeronautics and Space Administration is presently evaluating several parachutelike devices with gliding capability by means of wind-tunnel and flight tests. (For example, see refs. 1 to 5.)

The present wind-tunnel investigation is a continuation of this study and was undertaken to determine the aerodynamic characteristics of a twin-keel parawing configuration. The twin-keel parawing is a refined version of the earlier all-flexible single-keel parawing reported in references 1 and 2. The refinements include the addition of a

rectangular center panel to increase the aspect ratio of the basic single-keel configuration and the contouring of the nose portion of the center panel to produce an airfoillike leading edge. The investigation consisted of wind-tunnel static force tests using two different testing techniques. The performance characteristics were determined from tests in which the model was tethered by the suspension lines to a fixed mounting bar and allowed to "fly" freely in the airstream. During these tests the trim angle of the parawing was changed by varying the length of the aft-keel and wing-tip lines. To obtain longitudinal and lateral stability and control characteristics, tests were conducted using a center-post apparatus which supported the model at the confluence of the suspension lines and at the canopy. The apparatus allowed the parawing to be moved from its trim position and measurements of the aerodynamic forces and moments to be made at other than trimmed conditions. The tests were conducted over a range of angle of attack from the lowest value attainable without nose collapse to a value corresponding to the vertical descent condition and over a range of sideslip angle from 10° to -10°. Both the tether and the center-post tests were conducted at a dynamic pressure of about 1.0 pound/foot^2 (47.9 N/m^2) in the Langley full-scale tunnel.

SYMBOLS

The data are referred to the stability system of axes. The origin of the axes was located to correspond to a center-of-gravity position at the confluence point of the suspension lines. The coefficients are based on the laid-out-flat canopy area of 173.7 feet^2 (16.14 m^2), keel length of 15 feet (4.57 m), and wing span of 23 feet (7.01 m). The units used for the physical quantities defined in this paper are given both in the U.S. Customary Units and in the International System of Units (SI). Factors relating the two systems are given in reference 6.

b wing span, feet (meters)

C_D drag coefficient, $\dfrac{D}{qS}$

C_L lift coefficient, $\dfrac{L}{qS}$

C_l rolling-moment coefficient, $\dfrac{\text{Rolling moment}}{qSb}$

$C_{l_\beta} = \dfrac{\partial C_l}{\partial \beta}$, per degree

C_m pitching-moment coefficient, $\dfrac{\text{Pitching moment}}{qSl_k}$

2

C_n yawing-moment coefficient, $\dfrac{\text{Yawing moment}}{qSb}$

$C_{n_\beta} = \dfrac{\partial C_n}{\partial \beta}$, per degree

C_Y lateral-force coefficient, $\dfrac{\text{Lateral force}}{qS}$

$C_{Y_\beta} = \dfrac{\partial C_Y}{\partial \beta}$, per degree

D drag, pounds   (newtons)

F_A axial force, pounds   (newtons)

L lift, pounds   (newtons)

L/D lift-drag ratio

l length of suspension line, feet   (meters)

l_k keel length, feet   (meters)

M moment, foot-pounds   (meter-newtons)

q free-stream dynamic pressure, pounds/foot^2 (newtons/meter^2)

S wing area, feet^2 (meters^2)

W_c weight of canopy and lines, pounds   (newtons)

x distance from theoretical apex of model along leading edge or keel

x_1 distance between suspension-line confluence point and moment center of upper strain-gage balances of support system, feet   (meters)

x_2 distance between suspension-line confluence point and estimated center of gravity of canopy and suspension lines, feet   (meters)

α angle of attack (angle between relative wind and wing chord plane perpendicular to center post; center post defines a line from suspension-line confluence point to 0.60 keel point at the canopy), degrees

β angle of sideslip, degrees

Subscripts:

k-12   aft-keel lines

t   wing-tip lines

L-6   left wing-tip line

R-6   right wing-tip line

APPARATUS AND TESTS

Model

Drawings of the canopy of the model in a laid-out-flat condition are presented in figure 1. Photographs of the model mounted for testing in the Langley full-scale tunnel are presented in figures 2 and 3. The twin-keel parawing is essentially a single-keel parawing configuration with a rectangular panel added to form a center section between the triangular outboard panels. The nose section of the model was contoured to form an airfoil-shaped leading edge. Construction details of the nose section are presented in figure 1(b). The model was made of rip-stop nylon cloth which had a unit weight of 1.6 ounces/yard^2 (0.0542 kg/m^2) with an acrylic coating which reduced the porosity to less than 10 feet^3/minute (0.0047 m^3/sec) at a pressure of 10 inches (25.4 cm) of water. The model had 36 suspension lines of 250-pound (1112 N) test hot-stretched dacron, 12 along each keel, and 6 along each leading edge. (See fig. 1(b) for line spacing and length.) Changes in length of the aft-keel lines were used as a pitch control and differential changes in length of the wing-tip lines were used as a lateral-directional control.

Tether Test Setup

The tether test arrangement used in the investigation is shown in figure 2. The parawing suspension lines were attached to a T-shaped mounting bar (fig. 4) that was fixed to the full-scale-tunnel mechanical scale system. In order to insure stability of the unconstrained model, the aft-keel lines were spread longitudinally from the common attachment point of the suspension lines at the base of the T to the top center of the mounting bar and the wing-tip lines were spread laterally to the ends of the crossarm of the mounting bar. The lift and drag characteristics of the parawing were modulated by changing the lengths of aft-keel and wing-tip lines. The tests were limited to control

4

positions between those that reduced the angle of attack to the point of nose collapse and those that increased the angle of attack to the point at which the model became unstable.

Center-Post Test Setup

The center-post test apparatus used in the present investigation is essentially the same force-test system used and described in detail in references 1 and 5 with modifications made to accommodate the twin-keel parawing configuration. A sketch showing the test setup is presented in figure 5. The apparatus was designed to support the model at the confluence point of the lines and at the canopy and to provide a means for measuring the forces and moments produced when the configuration was forced to an out-of-trim condition. With this test setup, the model was restrained in roll, pitch, and yaw in such a way that fabric distortion was minimized and line stretch was virtually unaffected. The basic length of the aft-keel lines was increased from $l/l_k = 0.876$ to 0.912 to compensate for moving the lines from the spread position of the tether tests to the single confluence of the constrained tests. The wing-tip lines were also moved to the common attachment point but were shortened from a basic length of $l/l_k = 0.695$ to 0.670 in an effort to improve the aerodynamic performance of the configuration. (See fig. 1(b) for line lengths.)

Test Procedure

The tether tests were conducted to measure the aerodynamic performance of the twin-keel parawing as a function of various control-line settings. With the test technique, each data point represents a trimmed condition in the wind tunnel. These conditions, however, do not represent trimmed free-gliding flight exactly because the weight vector of the model as it is tested in the wind tunnel acts aft of the center of gravity of the configuration (assumed in this study to be the confluence of the suspension lines) and not through the center of gravity as in free flight. It is believed that this method of testing in a horizontal wind tunnel does simulate, as nearly as possible, free-gliding flight because there are no strut members attached to the model which could cause shape distortions and aerodynamic interference. The test procedure consisted of measuring the lift and drag forces produced for a systematic variation of the aft-keel and wing-tip lines while the model was in tethered flight. Because there was some fluctuation of forces during the tests, a number of readings were taken at each condition and the average of these is presented as a data point.

The center-post tests were conducted primarily to measure the moments produced by the model in out-of-trim conditions in both angle of attack and sideslip and thus to provide a basis for establishing the static stability parameters of the configuration. Lift and drag were also measured during these tests, but no attempt was made to shape the

canopy by adjusting wing-tip and aft-keel lines to optimize lift-drag ratio. The center-post testing technique was also used to measure the moments resulting from changes in length of the control lines of the parawing.

The investigation was conducted in the Langley full-scale tunnel, a complete description of which is given in reference 7. The lift and drag characteristics of the model were determined from measurements obtained from the tunnel scale-balance system. These data were corrected for the aerodynamic tare of the center-post test apparatus but no attempt was made to correct for possible mutual interference effects between model and support. The pitching-moment characteristics were obtained from strain gages attached to the center post at the model canopy. The strain-gage measurements were used to eliminate the possible errors in pitching moment involved with small inaccuracies in force measurements when forces were transferred over the long moment-arm distances in the tunnel measurement system. The sketch presented as figure 6 shows how the forces and moments measured by the strain-gage balances were used to compute pitching-moment coefficient and how the pitching moment was corrected for the model weight component acting aft of the reference center of gravity and not through this point as in flight. An indication of the magnitude of the weight tare correction and a discussion of its effect on the static data are presented in reference 5. In the lateral tests the tunnel force-measuring system was used inasmuch as the model was not instrumented with strain gages to read lateral forces and moments.

Test Conditions

The tests were conducted at a dynamic pressure of 1.0 pound/foot^2 (47.9 N/m^2). The test Reynolds number based on the actual model keel length of 12 feet (3.66 m) was 2.3×10^6. The center-post data were obtained over a range of angle of attack from 25° to 90° and at angles of sideslip from -10° to 10°. The data are presented with no wind-tunnel jet-boundary corrections applied.

RESULTS AND DISCUSSION

Longitudinal Aerodynamic Characteristics

Performance.- The aerodynamic performance characteristics of the twin-keel parawing as determined from the tether tests are shown in figure 7. Lift coefficient, drag coefficient, and lift-drag ratio are presented as functions of incremental changes in the aft-keel lines from their basic length for various settings of the wing-tip lines. The data are for trimmed conditions in the horizontal wind tunnel and are limited in the low angle-of-attack range (low values of C_L) by nose collapse and in the high angle-of-attack range (high values of C_L) by model instability. Increasing the keel-line length is shown to result in a reduction of lift coefficient and an increase in L/D, except for

6

the tip-line lengths of $\Delta l_t/l_k$ = -0.033 and -0.058 for which L/D decreased at keel-line lengths greater than $\Delta l_{k-12}/l_k$ = 0.02 and 0.05, respectively. The reason for this loss in L/D was that the nose of the canopy collapsed with attendant large increases in drag. Except for these conditions where the nose of the canopy collapsed, changing the length of the tip lines had little effect on either lift or L/D.

Although the aft-keel- and wing-tip-line settings for maximum lift-drag ratio were not defined during the investigations, the slight change in L/D between the $\Delta l_t/l_k$ = -0.079 and -0.092 cases indicates that the value had about reached maximum for the present rigging. The maximum L/D value of 3.4 was obtained with the wing-tip lines set at $\Delta l_t/l_k$ = -0.092. Also presented in figure 7 are trimmed values of lift and drag taken from the center-post tests. Although there were configuration differences in the two test techniques (in the tether tests the aft-keel and wing-tip lines were spread from the single confluence to stabilize the model, in the center-post tests there were unknown interference effects of the support apparatus), the data show the same general trends. The center-post tests, which were made with different basic keel- and wing-tip-line settings (see fig. 1(b)), produced a maximum lift-drag ratio of 2.4. In general, the performance data from the tether tests indicate that the lift-drag ratio could be modulated from a minimum of 2.2 to 3.4 and lift coefficient could be modulated from 1.00 to about 0.70 for the range of line lengths used in the investigation.

Stability and control.- The longitudinal stability and control characteristics of the twin-keel parawing as determined from the center-post tests are presented in figure 8. Data are presented for three individual tests made under the same conditions, and the results indicate good repeatability over the entire test angle-of-attack range. The minimum angle of attack reached during these tests was 26°. At angles below this value, the nose would not remain inflated and tended to tuck under or the canopy would collapse completely. The maximum value of lift coefficient of about 1.08 occurred at an angle of attack of 40°. The maximum lift-drag ratio of 2.4 with the basic wing-tip-line length used in the center-post test arrangement occurred at 26°, the lowest angle of attack attainable. The pitching-moment data show that the model was longitudinally stable over an angle-of-attack range of 15° up to the stall angle (α = 40°) and was unstable over the remainder of the test angle-of-attack range.

The longitudinal stability characteristics of the twin-keel parawing are compared in figure 9 with those of the single-keel parawing configuration which were also determined from tests using the center-post apparatus and are reported in reference 1. As may be seen, the configurations had similar longitudinal stability characteristics — stability in the low angle-of-attack range and an unstable break in the pitching-moment curve at the stall angle. It may also be noted that unlike the single-keel model, the twin-keel configuration was tested at angles of attack well below the stall. This characteristic of

the twin-keel model to "fly" on the "front," or unstalled, side of the lift curve, which is probably a result of the contoured nose section, allows the possibility of some modulation of lift coefficient in the stable angle-of-attack range and also permits the angle of attack for maximum lift-drag ratio to be more nearly realized. The twin-keel model had higher values of lift and lower values of drag with resultant greater values of lift-drag ratio over most of the angle-of-attack range. Although direct comparison of lift and drag is valid only for the particular line configurations investigated, it is believed that the variation of the coefficients with angle of attack is representative for the two parawing models and that the twin-keel parawing will have higher values of lift-drag ratio.

The effect of changes in length of the aft-keel lines of the twin-keel parawing as a pitch control is presented in figure 10. These data indicate that the model was capable of being trimmed over the stable angle-of-attack range. This trim range allowed a variation in lift coefficient from about 0.87 to 1.07 and a variation in lift-drag ratio from 2.4 to 1.6.

Lateral Stability Characteristics

Because of the restraint imposed by the model-support spikes attached to strain-gage balances, which passed through the canopy at two spanwise positions (see fig. 5), the model could be held at various angles of sideslip. Whether or not the model could attain these angles in free flight and what deformations might occur are unknown. The lateral stability data are therefore only gross or qualitative indications of lateral stability. The lateral-stability tests were limited to a maximum angle of attack of 70° because of large constant-amplitude oscillations of the model when it was sideslipped at higher angles of attack. This occurrence, however, does not indicate that the wing would behave in this manner at angles of sideslip in free flight. The oscillation was very likely associated with the restraint provided by the mounting system.

The lateral stability characteristics are presented in figure 11 as the variation of the static lateral stability coefficients of the model with angle of sideslip for angles of attack from 30° to 70°. As may be seen, the data points form relatively smooth curves at angles of attack below the stall. At the stall angle, $\alpha = 40^{\circ}$, the data become irregular and, as would be expected, remain irregular over the stalled angle-of-attack range. These data are summarized in figure 12 in the form of the variation of the stability derivatives C_{Y_β}, C_{n_β}, and C_{l_β} with angle of attack. The values of the stability derivatives were obtained from the slopes of the curves in figure 11 through $\beta = 0^{\circ}$. Because of the irregularities of the data, especially at the higher angles of attack, the stability derivatives are only generally indicative of the characteristics of the configuration. These data show that the model had positive values of directional stability $\left(+C_{n_\beta}\right)$ and positive effective dihedral $\left(-C_{l_\beta}\right)$ that decreased to zero at about $\alpha = 40^{\circ}$. In the angle-of-attack

8

range from about 40° to 58° the parawing was directionally unstable and had negative effective dihedral. These unstable characteristics are related to the change in the sign of the lateral derivative C_{Y_β} since this parameter multiplied by its moment arm contributes significantly to directional stability and effective dihedral characteristics with respect to the low center-of-gravity position of the model. These lateral stability characteristics of the twin-keel parawing are very similar to those of the single-keel model reported in reference 1.

The effect of differential changes in the length of the wing-tip lines for lateral control is presented in figure 13 for both right and left controls at zero sideslip. Although the model had some asymmetry in the rigging, the data show that the forces and moments produced by either deflection, with the exception of sign, had generally similar variation with angle of attack. The difference between the values for left and right controls was divided by 2 to give average control characteristics for the system. The results are shown in figure 14 as the incremental lateral force and moment coefficients produced by a right-wing-down control. For this configuration, positive (right) rolling moments and negative (left) yawing moments were produced over the test range of angle of attack. These characteristics are again similar to those of the single-keel parawing of reference 1.

SUMMARY OF RESULTS

The results of the full-scale tunnel investigation of the low-speed aerodynamic characteristics of a twin-keel parawing configuration may be summarized as follows:

1. The model had a maximum lift-drag ratio of 3.4.

2. The model was longitudinally stable from the minimum angle of attack attainable before nose collapse up to the stall angle, an angle-of-attack range of about 15°.

3. Changing the length of the aft-keel and wing-tip lines was effective in trimming the model over the entire unstalled angle-of-attack range and resulted in a modulation in lift-drag ratio from 2.2 to 3.4.

4. The model was directionally stable and had positive effective dihedral over the unstalled angle-of-attack range. At angles of attack above the stall, however, the model became directionally unstable and had negative effective dihedral.

9

5. Differential deflection of the wing tips for lateral control produced positive rolling moments and negative yawing moments over the test range of angle of attack when the lines were changed in a direction to lower the right wing tip.

Langley Research Center,
  National Aeronautics and Space Administration,
    Langley Station, Hampton, Va., February 28, 1969,
   124-07-03-20-23.

REFERENCES

1. Libbey, Charles E.; Ware, George M.; and Naeseth, Rodger L.: Wind-Tunnel Investigation of the Static Aerodynamic Characteristics of an 18-Foot (5.49-Meter) All-Flexible Parawing. NASA TN D-3856, 1967.

2. Naeseth, Rodger L.; and Fournier, Paul G.: Low-Speed Wind-Tunnel Investigation of Tension-Structure Parawings. NASA TN D-3940, 1967.

3. Weiberg, James A.; and Mort, Kenneth W.: Wind-Tunnel Tests of a Series of Parachutes Designed for Controllable Gliding Flight. NASA TN D-3960, 1967.

4. Burk, Sanger M., Jr.; and Ware, George M.: Static Aerodynamic Characteristics of Three Ram-Air-Inflated Low-Aspect-Ratio Fabric Wings. NASA TN D-4182, 1967.

5. Ware, George M.; and Libbey, Charles E.: Wind-Tunnel Investigation of the Static Aerodynamic Characteristics of a Multilobe Gliding Parachute. NASA TN D-4672, 1968.

6. Mechtly, E. A.: The International System of Units – Physical Constants and Conversion Factors. NASA SP-7012, 1964.

7. DeFrance, Smith J.: The N.A.C.A. Full-Scale Wind Tunnel. NACA Rep. 459, 1933.
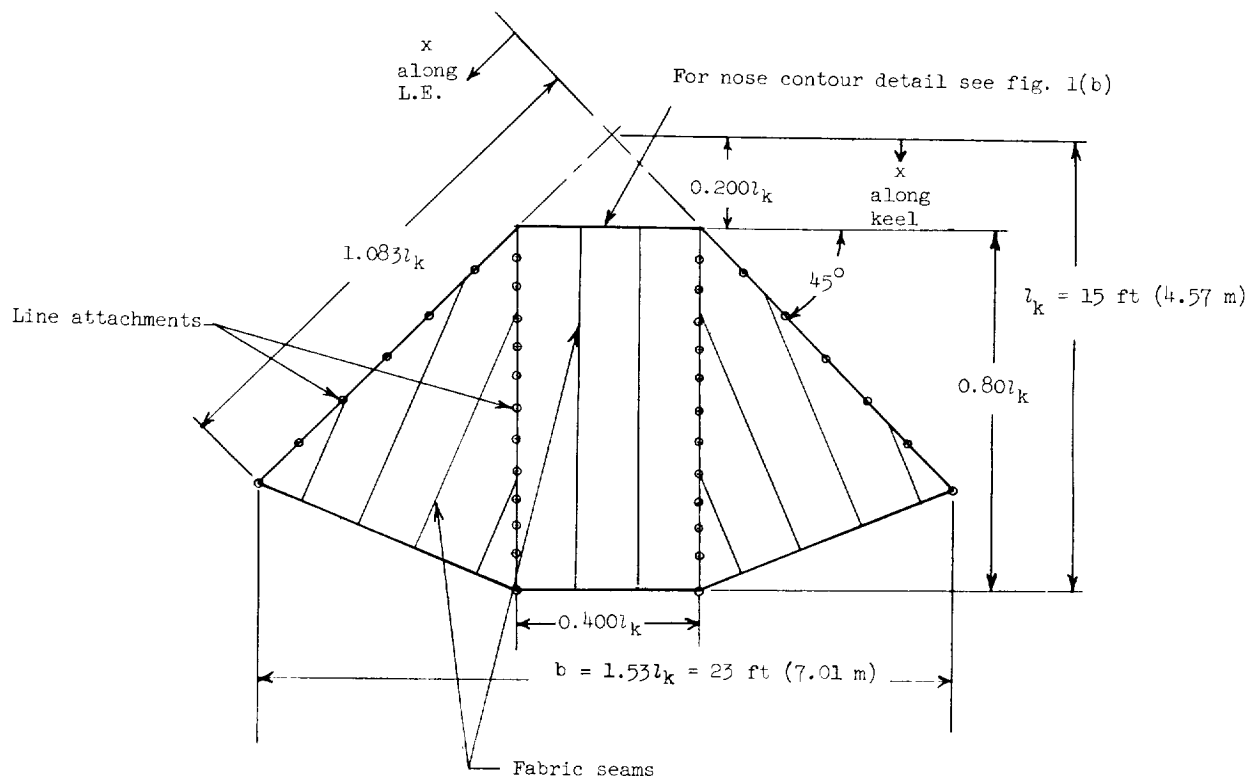
(a) Flat planform view.

Figure 1.- Sketches of twin-keel parawing used in investigation.
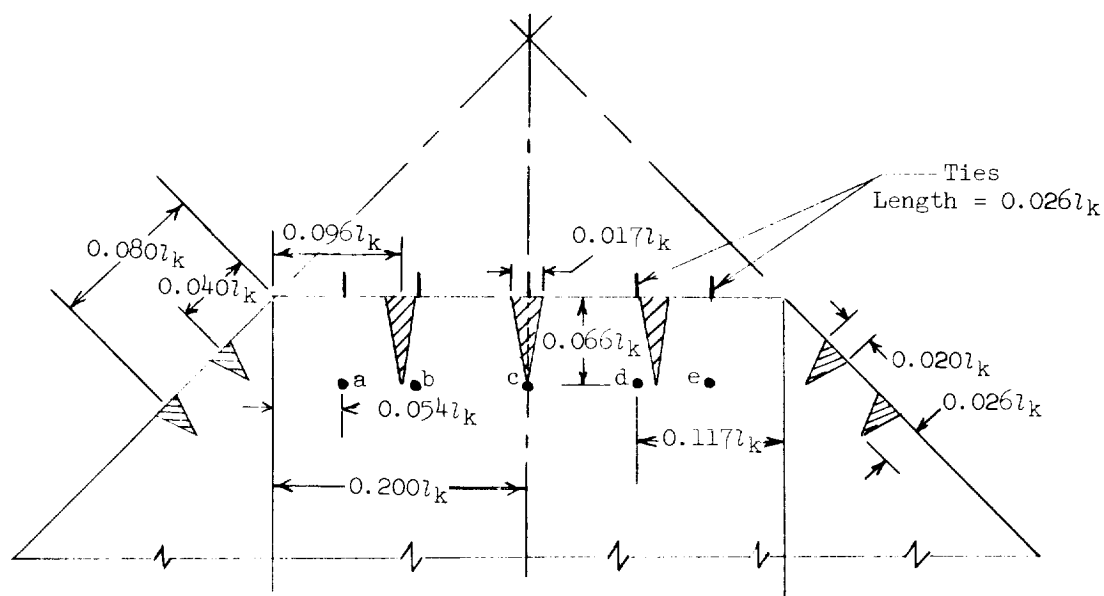
Note: Material indicated by shaded areas removed and fabric sewed.
Nose folded under and attached by ties at points a to e.

Line	Attachment location, x/l_k		Basic length, l/l_k	
	Keel	Leading edge	Keel	Leading edge
1	0.267	0.416	0.973	0.930
2	.333	.549	.987	.910
3	.400	.683	.980	.890
4	.466	.816	.979	.840
5	.533	.949	.978	.780
6	.600	1.083	.975	[a].695 (0.670)
7	.666		.960	
8	.733		.958	
9	.799		.957	
10	.866		.953	
11	.933		.930	
12	1.000		[a].876 (0.912)	

[a]Parenthetical values used with center-post tests.

(b) Nose contour detail and suspension line geometry.

Figure 1.- Concluded.
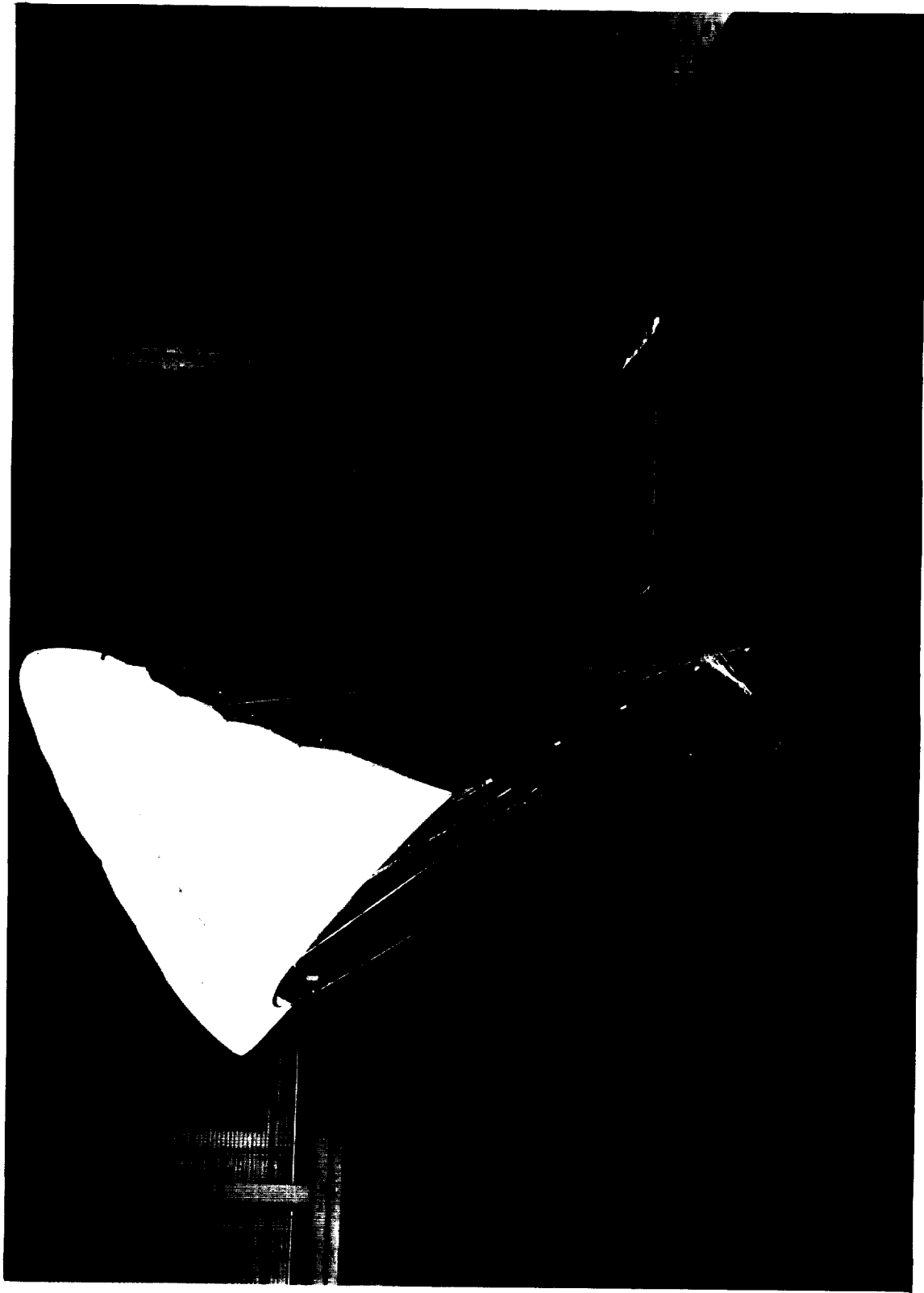
Figure 2.- Model mounted for tether tests in Langley full-scale tunnel.

L-67-9056

13
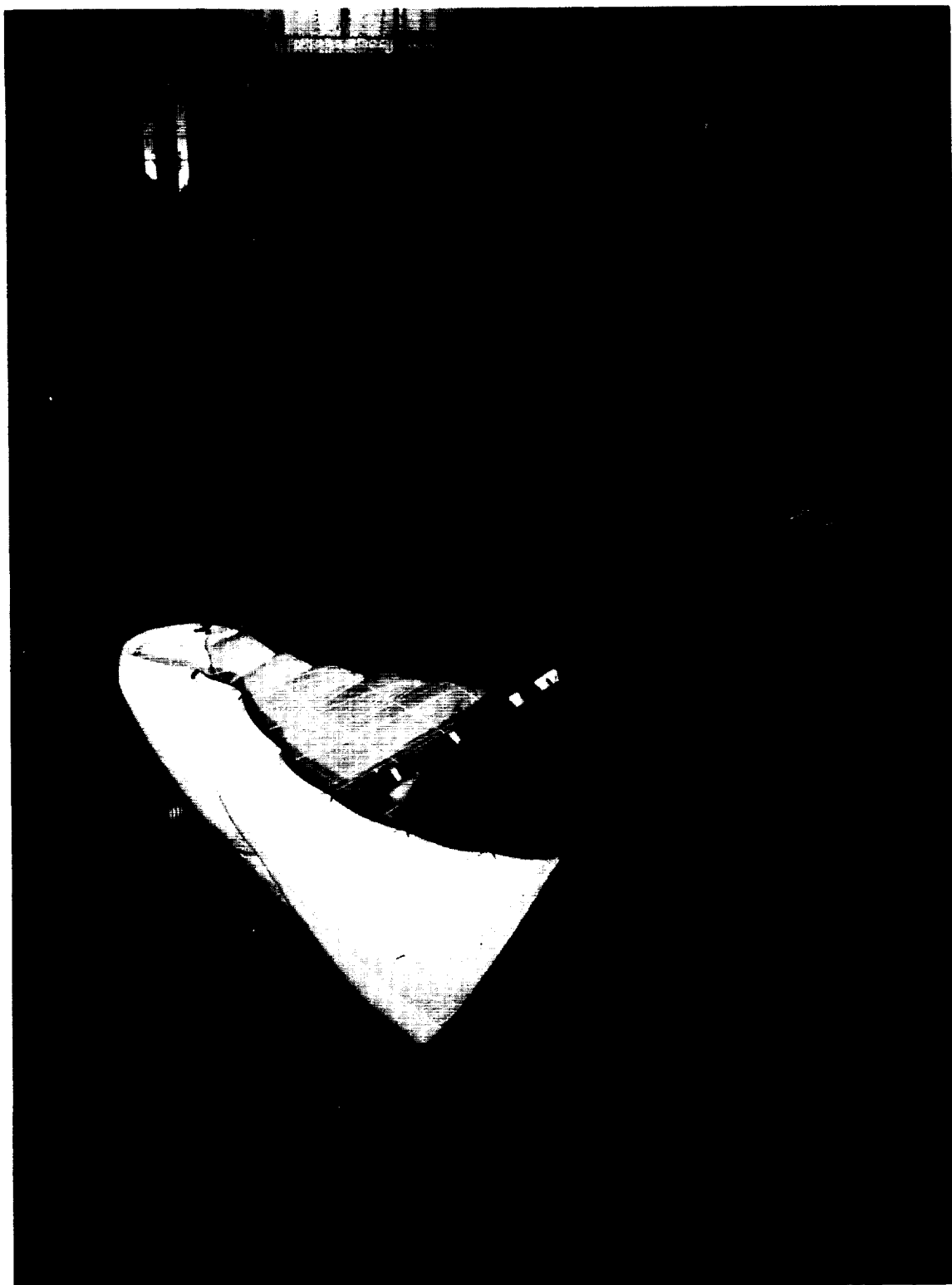
Figure 3.- Model mounted for center-post tests in Langley full-scale tunnel.

Wing-tip line attachment

Aft-keel lines attachment

Suspension lines confluence attachment

24.12
(61.26)

Wing-tip line
attachment

1.75
(4.45)

20.34
(51.66)
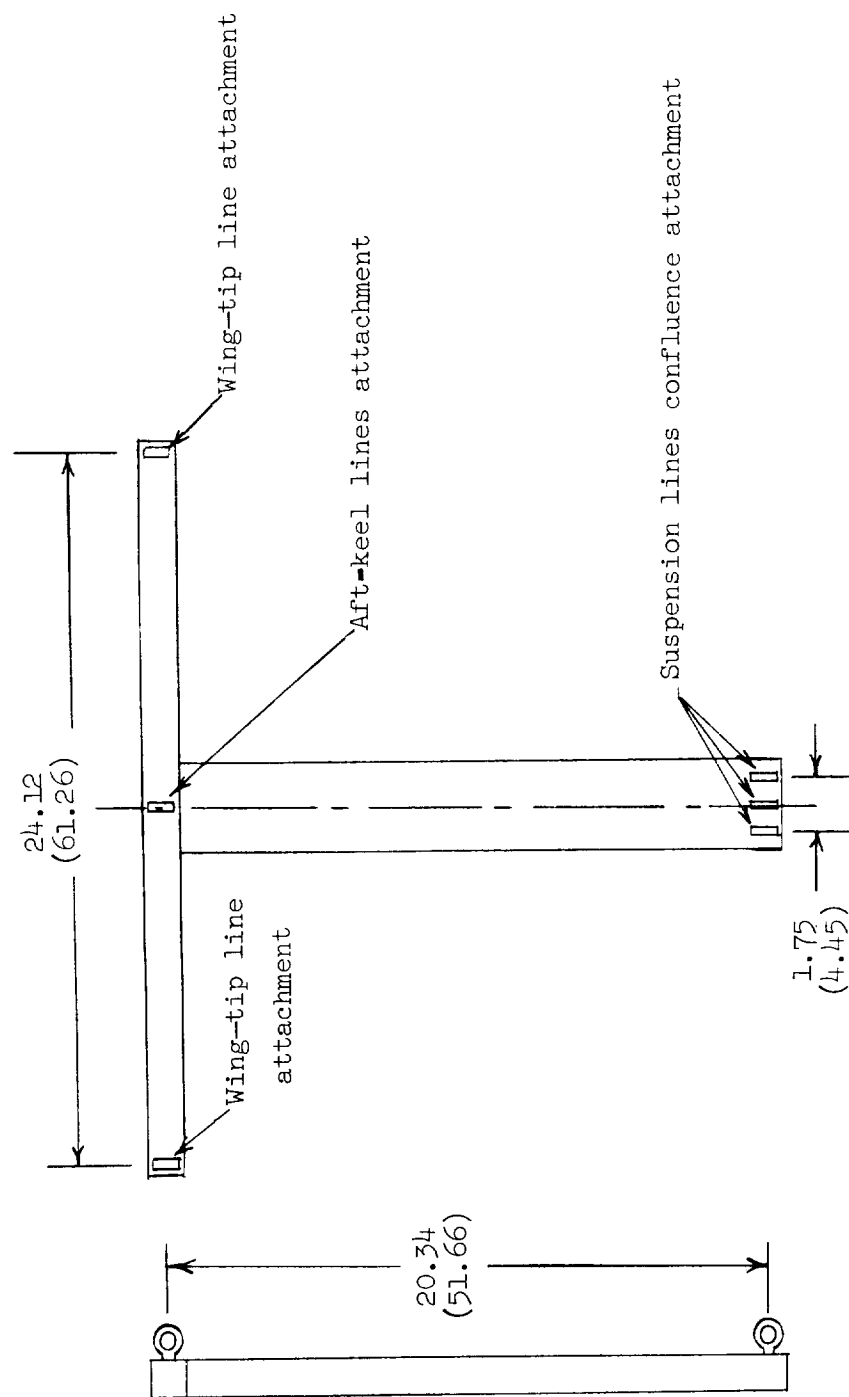
Figure 4.- Sketch of T bar fitting used in tether tests. All dimensions are in inches (centimeters).

15

Strain-gage balances

Angle-of-attack actuator

Center post

Support strut

Turntable attached to tunnel
force-measuring system
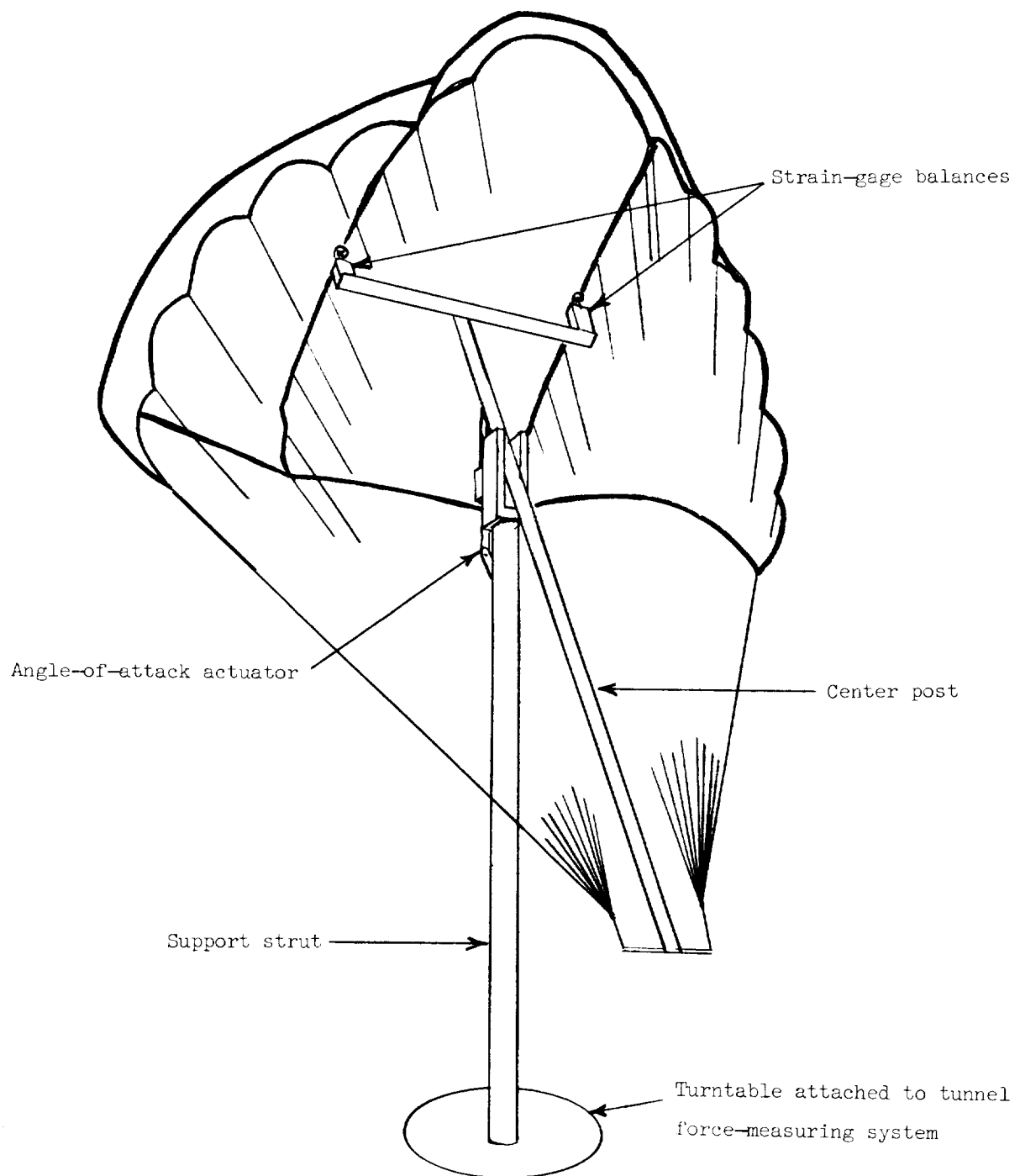
Figure 5.- Drawing showing center-post force-test apparatus in Langley full-scale tunnel.

16

$$W_c = 4.5 \text{ lb } (20.0 \text{ N })$$

$$x_1 = 13.9 \text{ ft } (4.2 \text{ m })$$

$$x_2 = 11.4 \text{ ft } (3.5 \text{ m })$$

$$C_m = \frac{M + F_A(x_1)}{qSl_k} - \frac{W_c(x_2)\sin\alpha}{qSl_k}$$
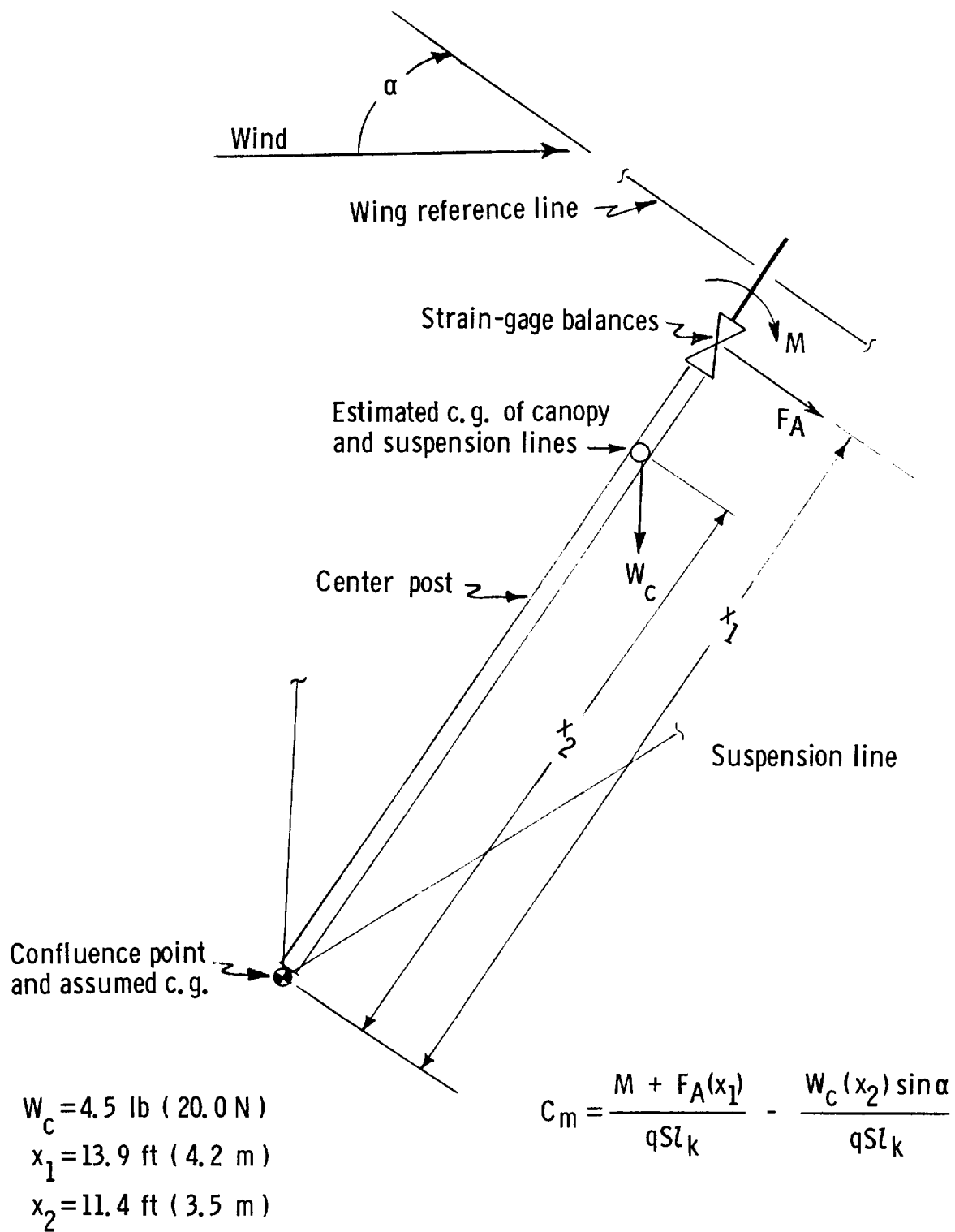
Figure 6.- Sketch showing how forces and moments at canopy were resolved into pitching moment.
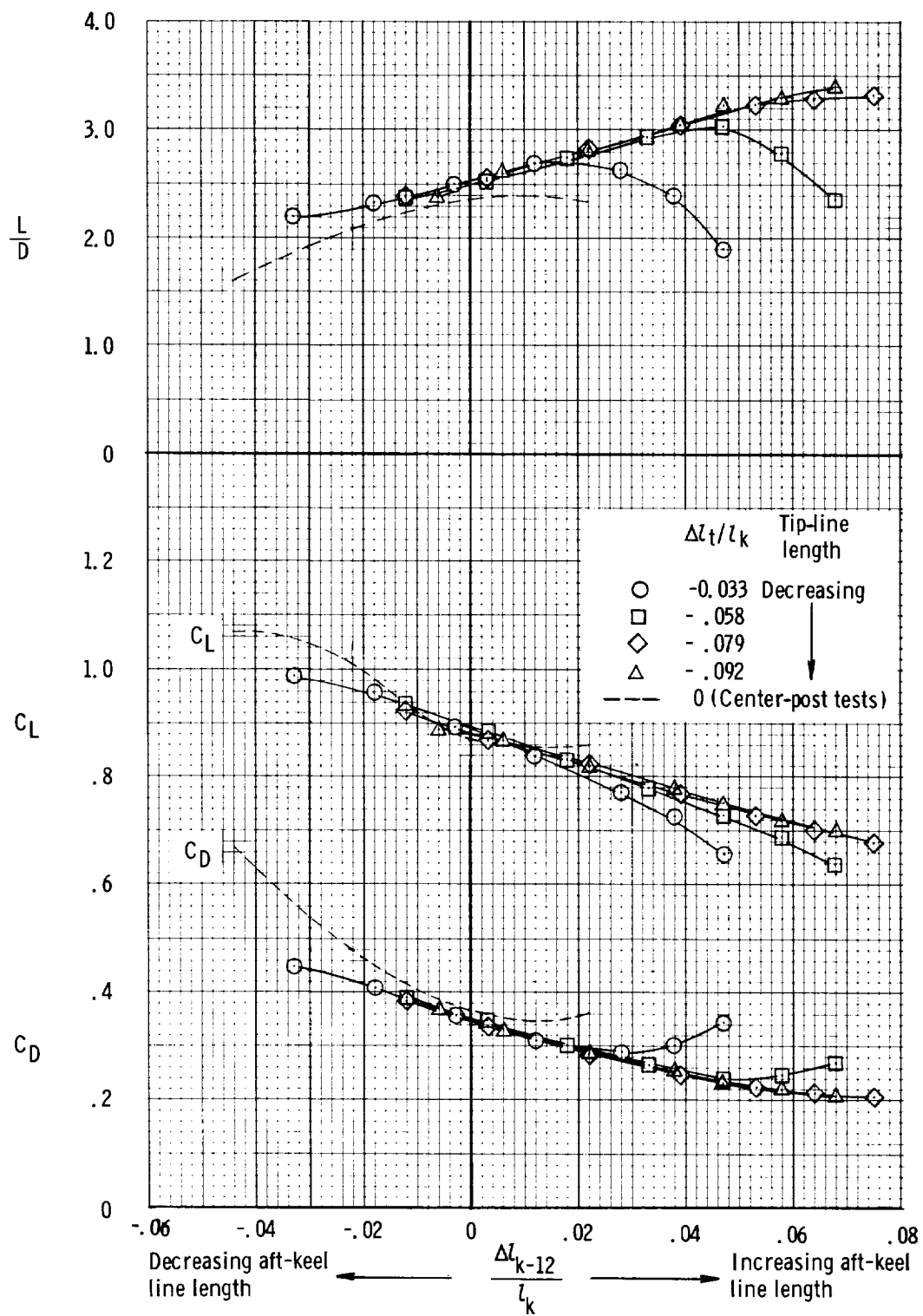
Figure 7.- Effect of variation of wing-tip and aft-keel lines on longitudinal performance characteristics of model. $C_m = 0$; $\beta = 0^0$.
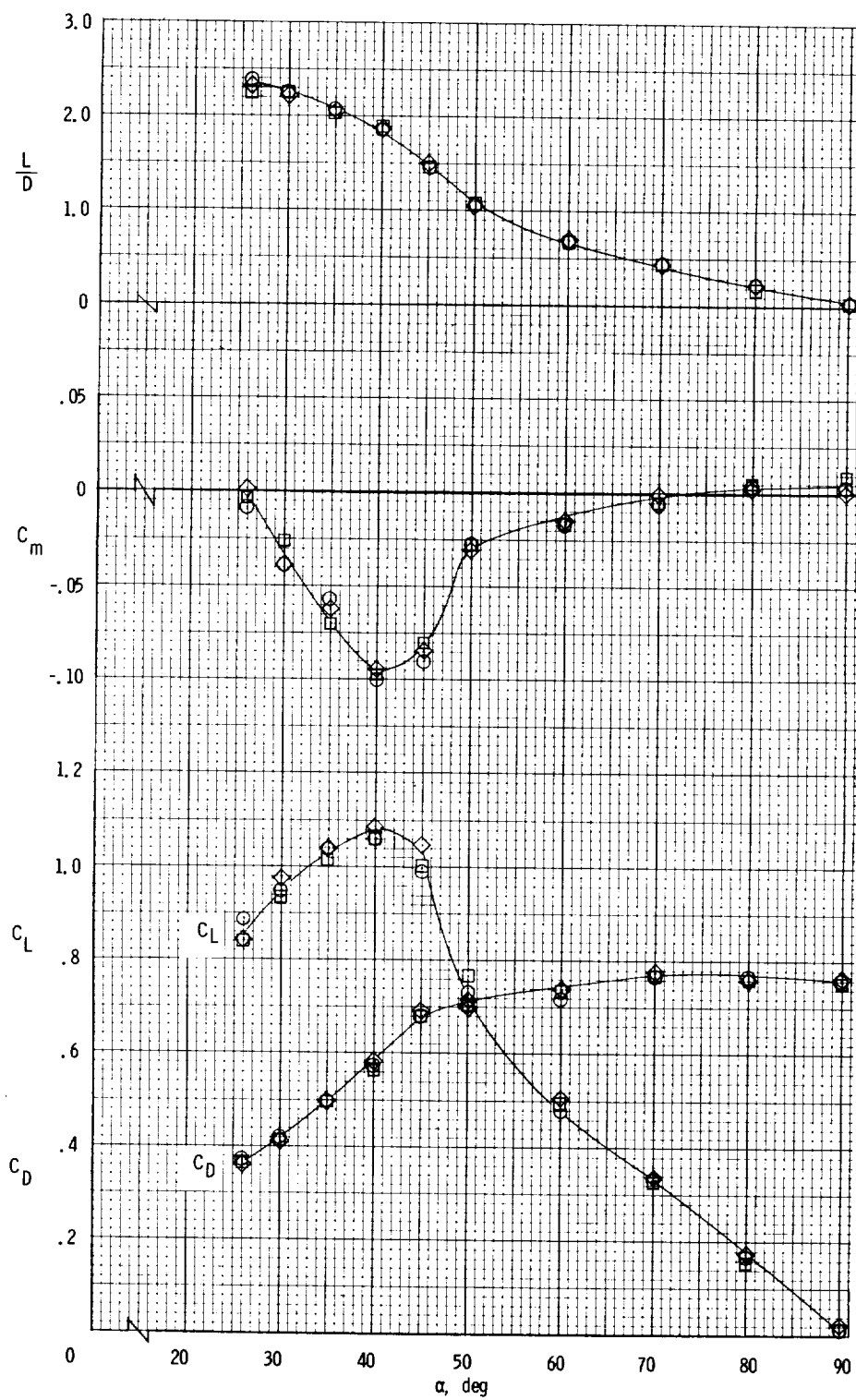
Figure 8.- Longitudinal stability characteristics of twin-keel parawing. $\beta = 0^0$. Different symbols represent different tests and show repeatability of data.
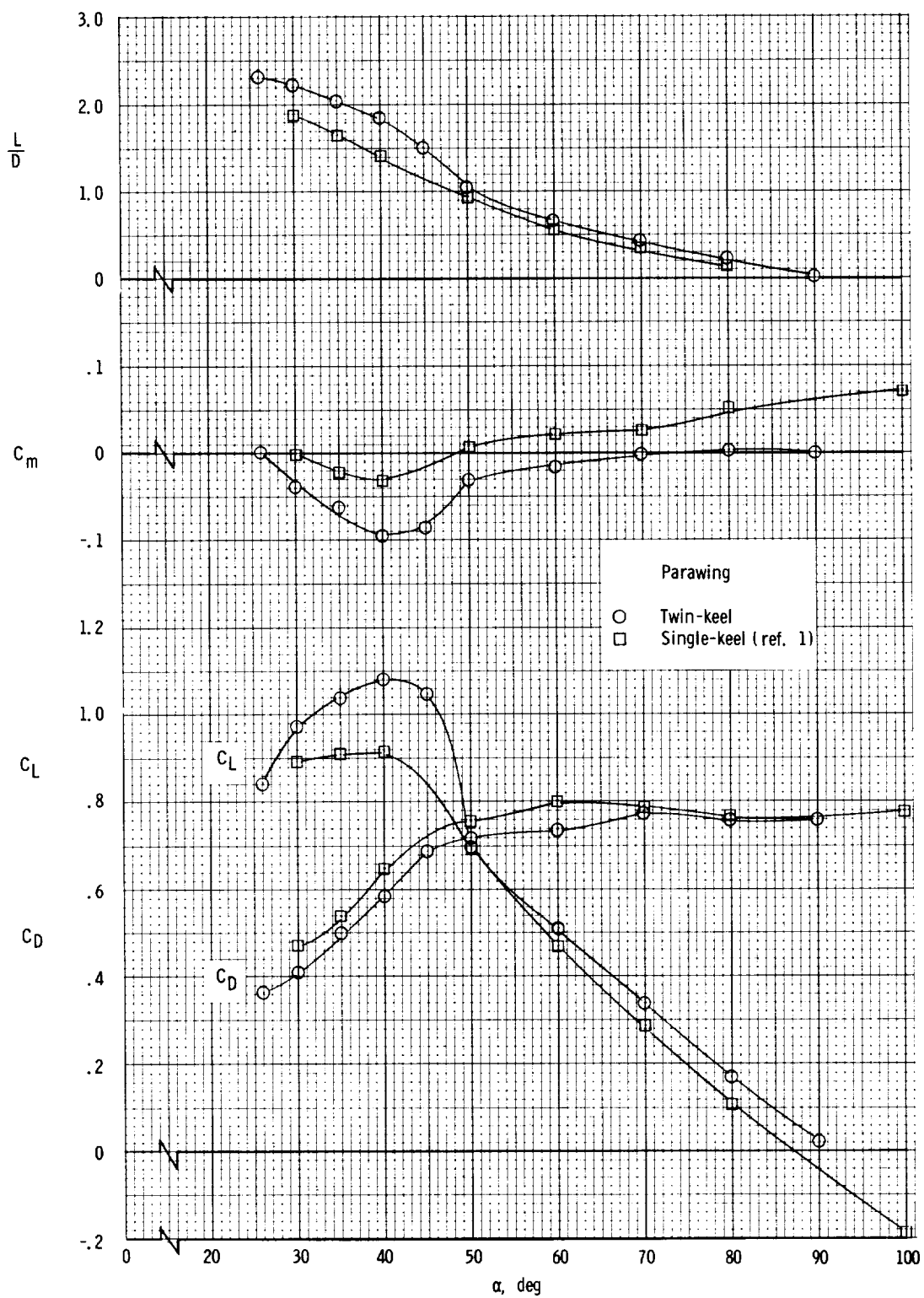
Figure 9.- Comparison of longitudinal stability characteristics of single- and twin-keel parawings. $\beta = 0^0$.
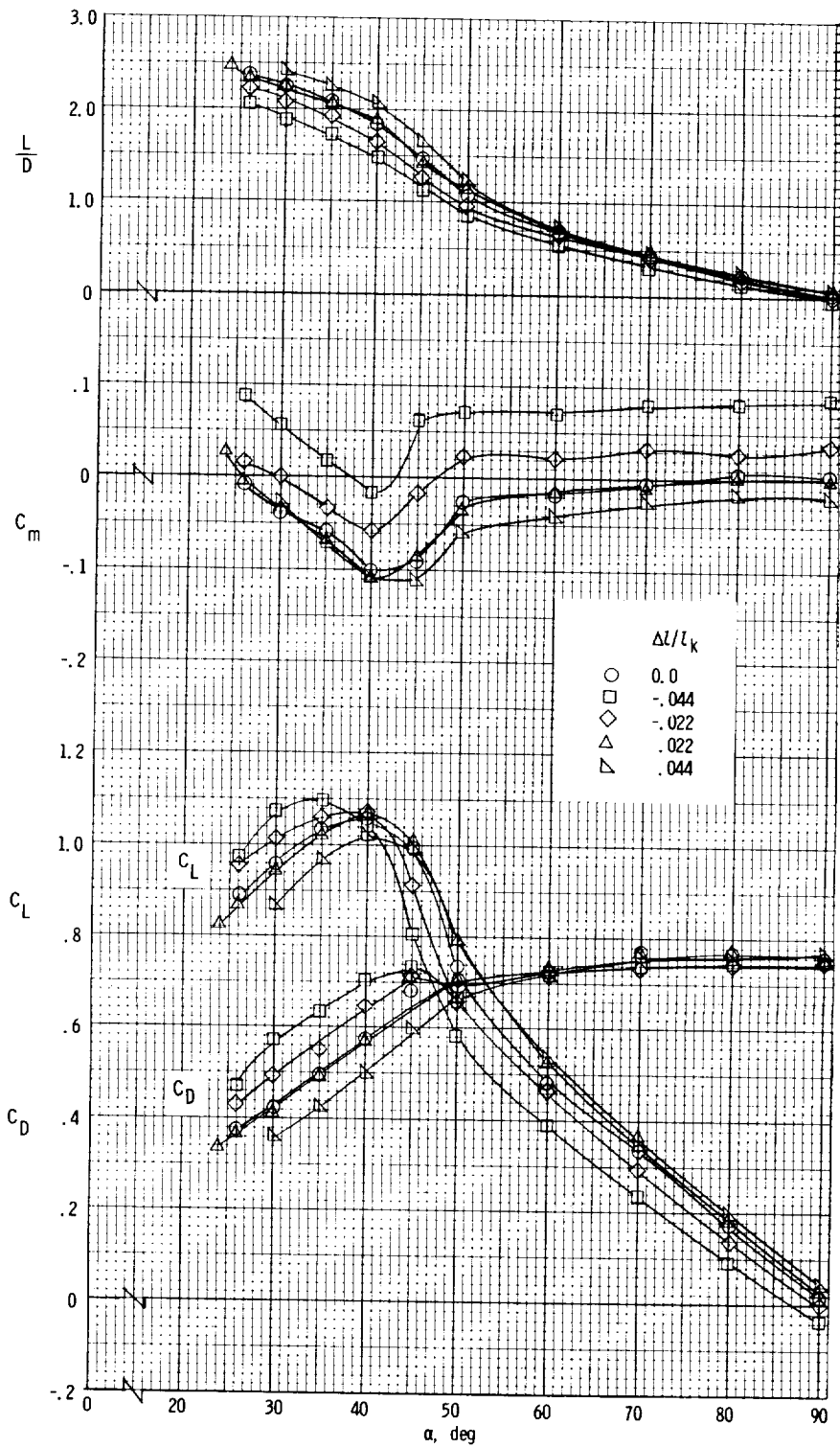
Figure 10.- Effect of changes in length of aft-keel lines for pitch control. $\beta = 0^{o}$.

(a) α = 30⁰.   (b) α = 35⁰.
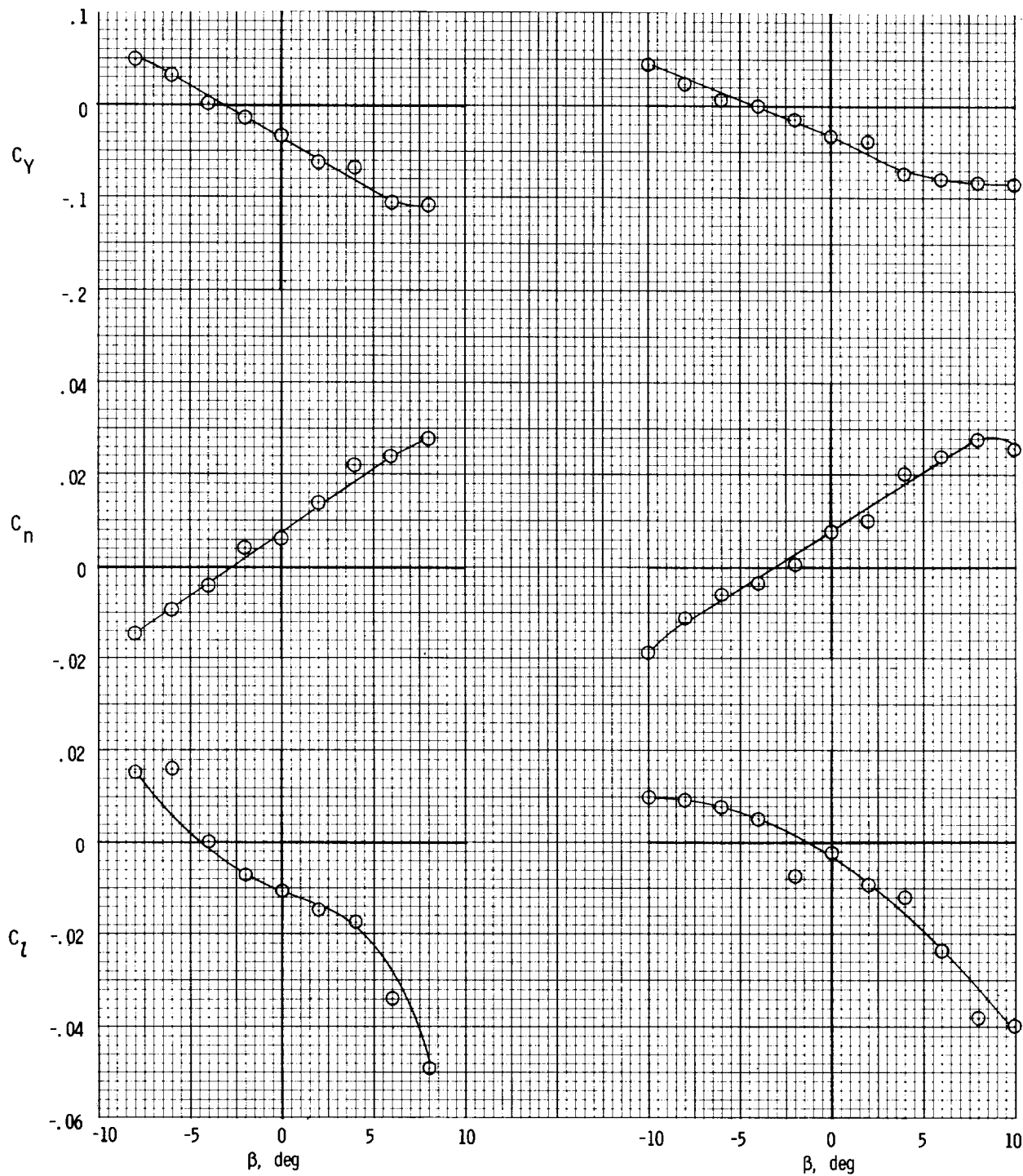
Figure 11.- Variation of lateral stability coefficients with angle of sideslip.

(c) $\alpha = 40^0$.　　　　　(d) $\alpha = 45^0$.

Figure 11.- Continued.

23

(e) α = 50⁰.

(f) α = 60⁰.

Figure 11.- Continued.

24
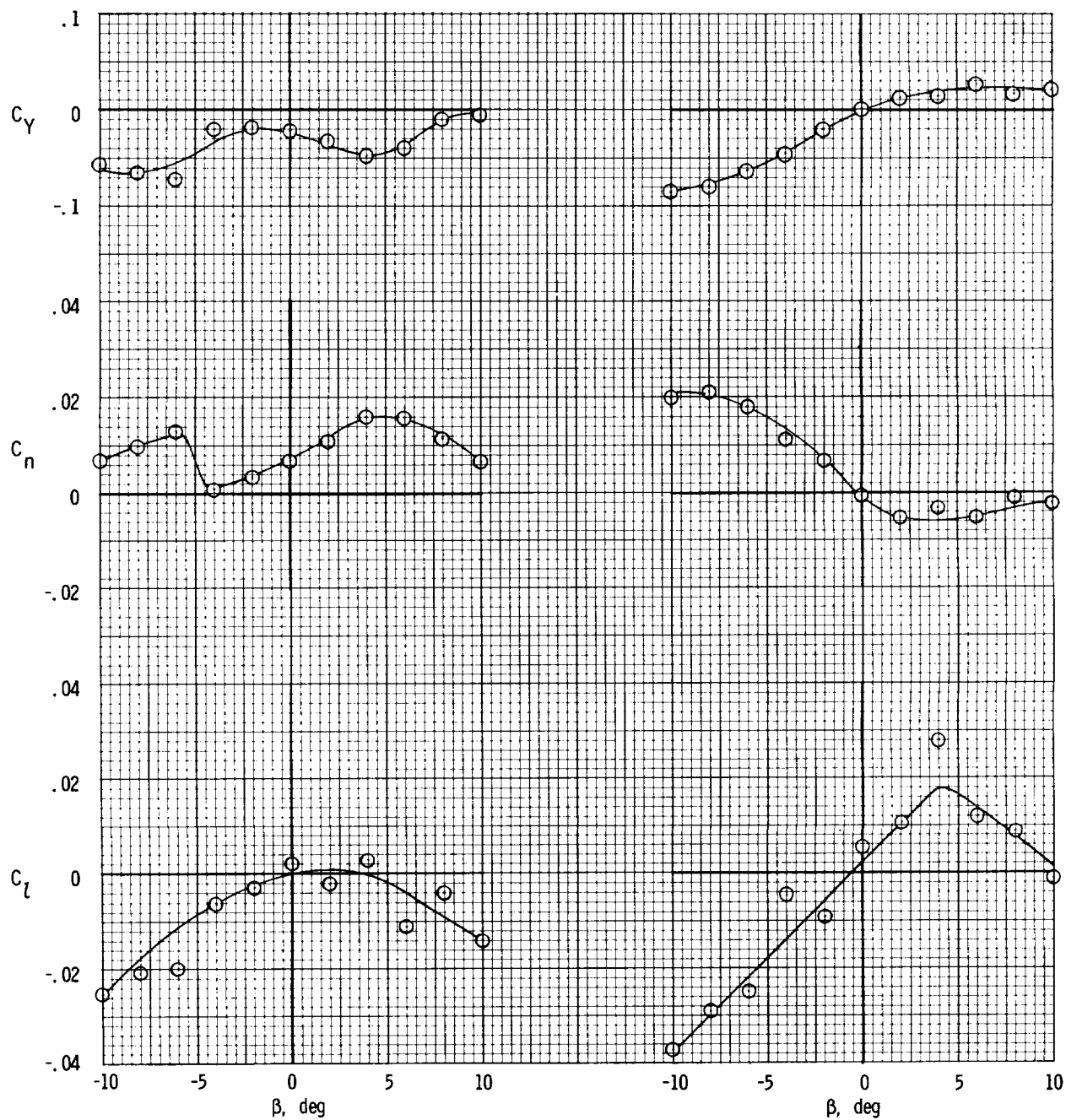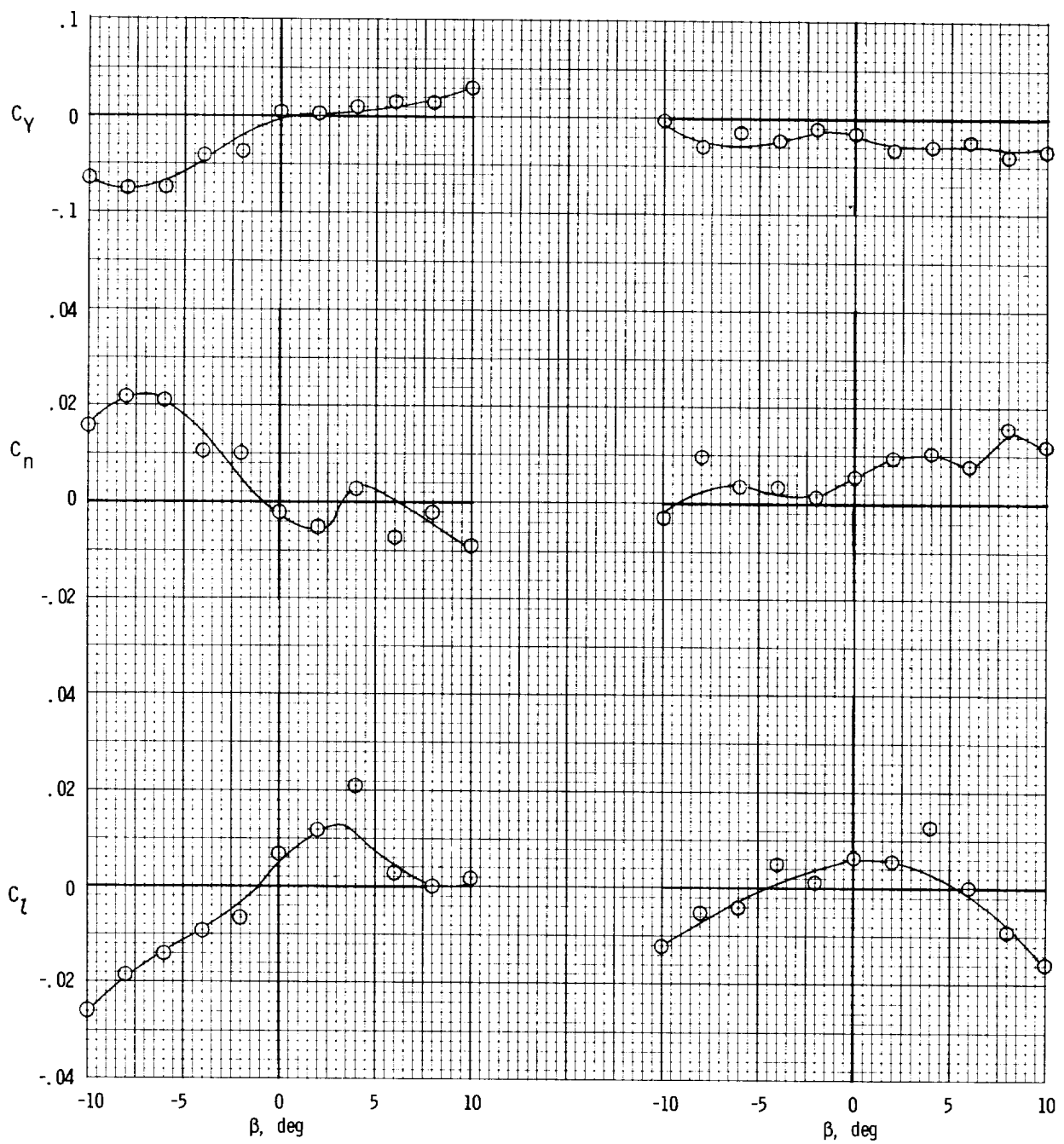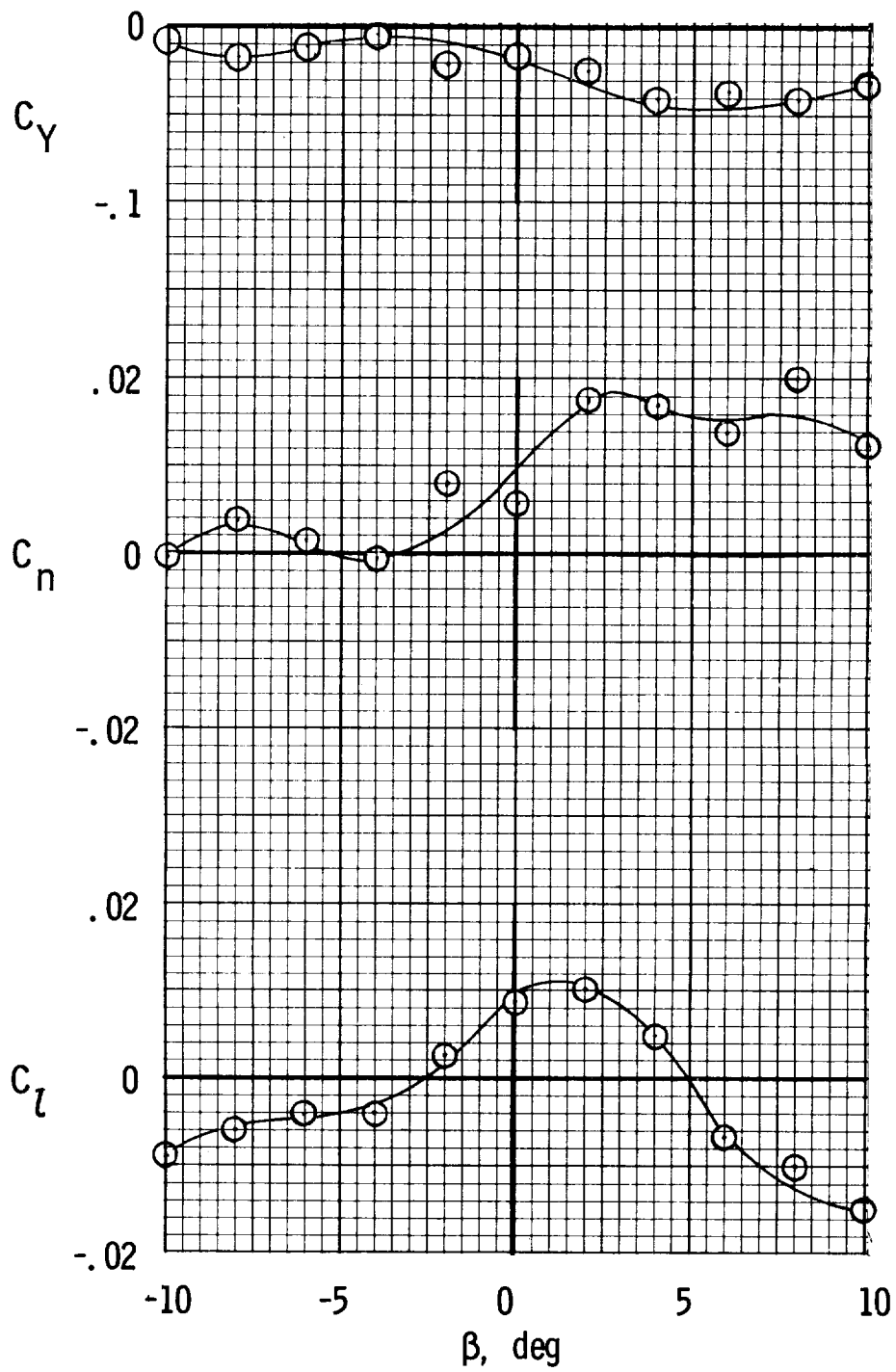
(g) $\alpha = 70^{\circ}$.

Figure 11.- Concluded.
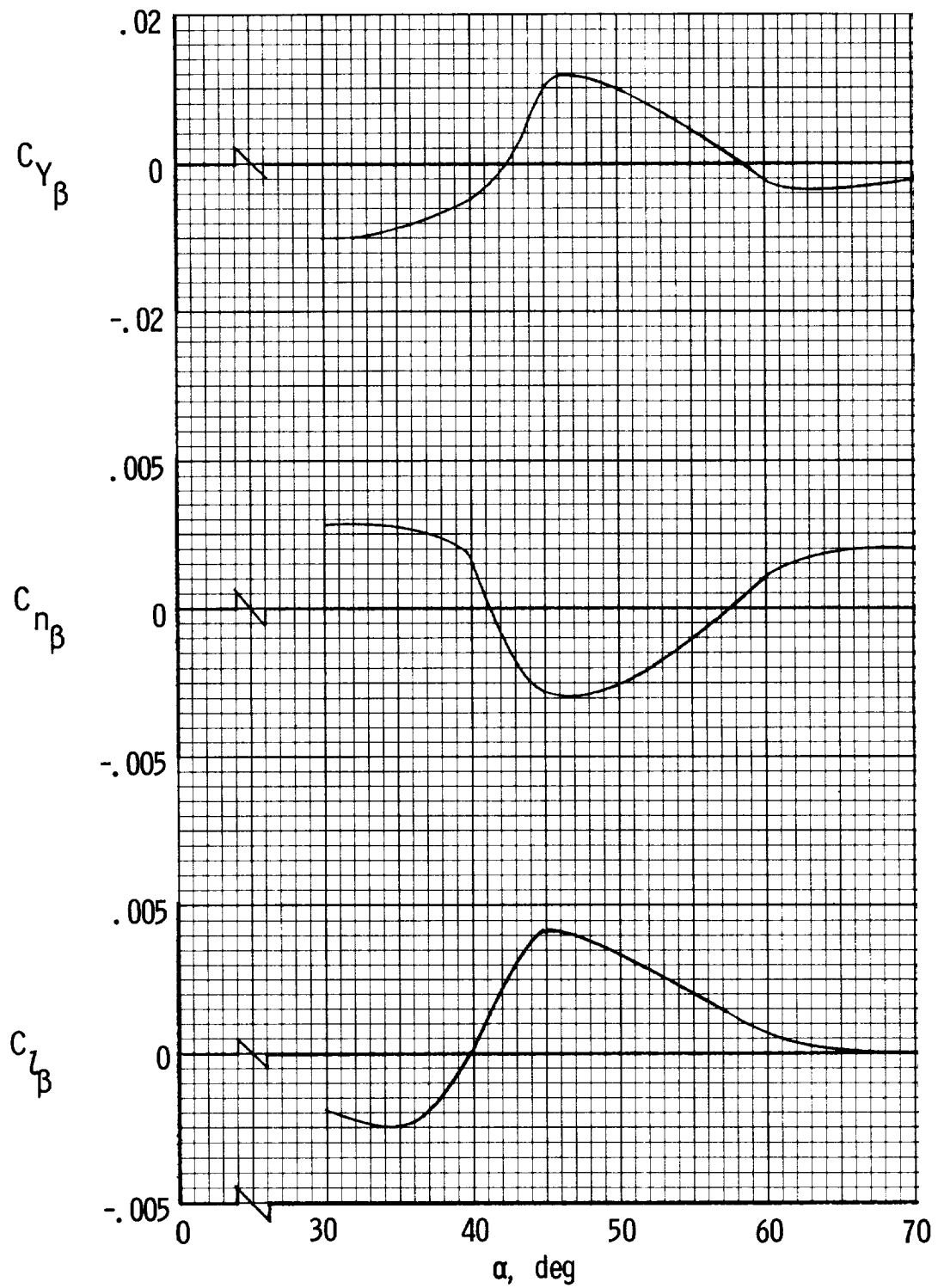
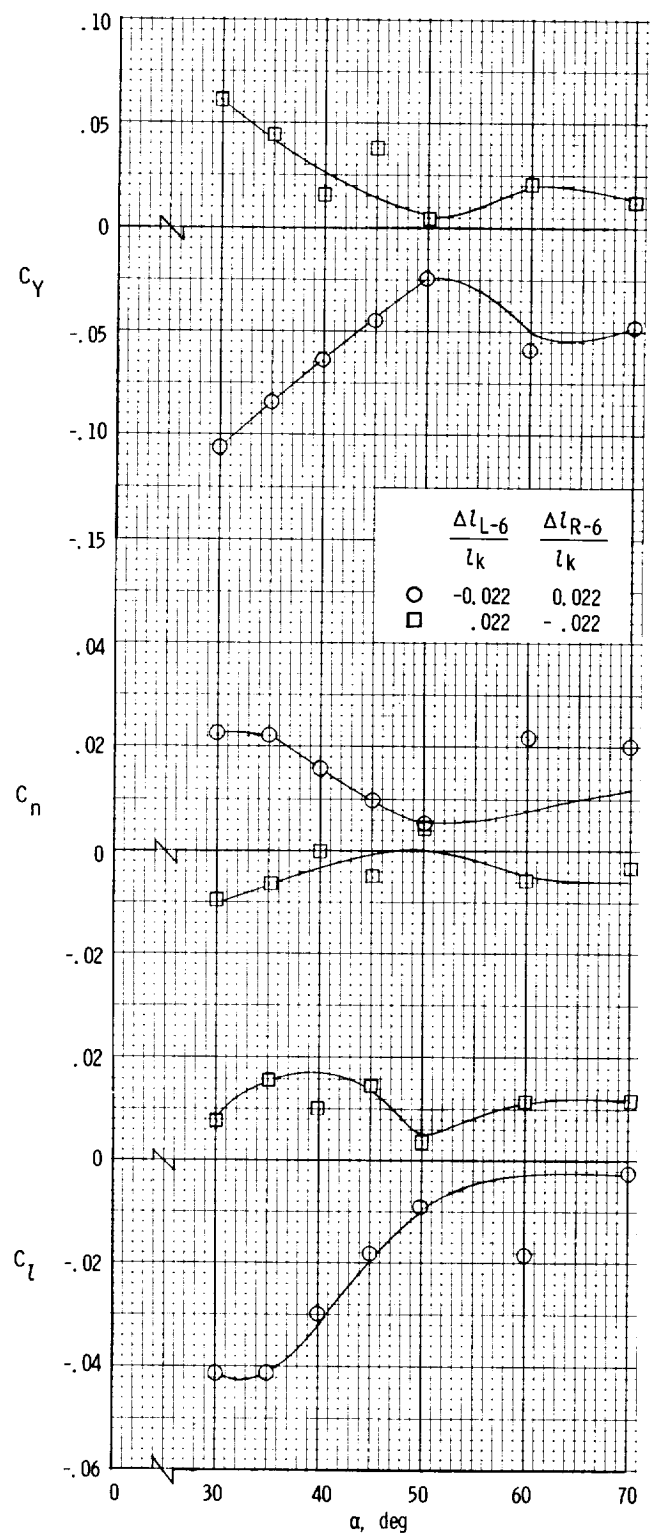Figure 12.- Lateral stability characteristics of model.

Figure 13.- Effect of differential wing-tip deflection on lateral stability characteristics of model. $\beta = 0^\circ$.
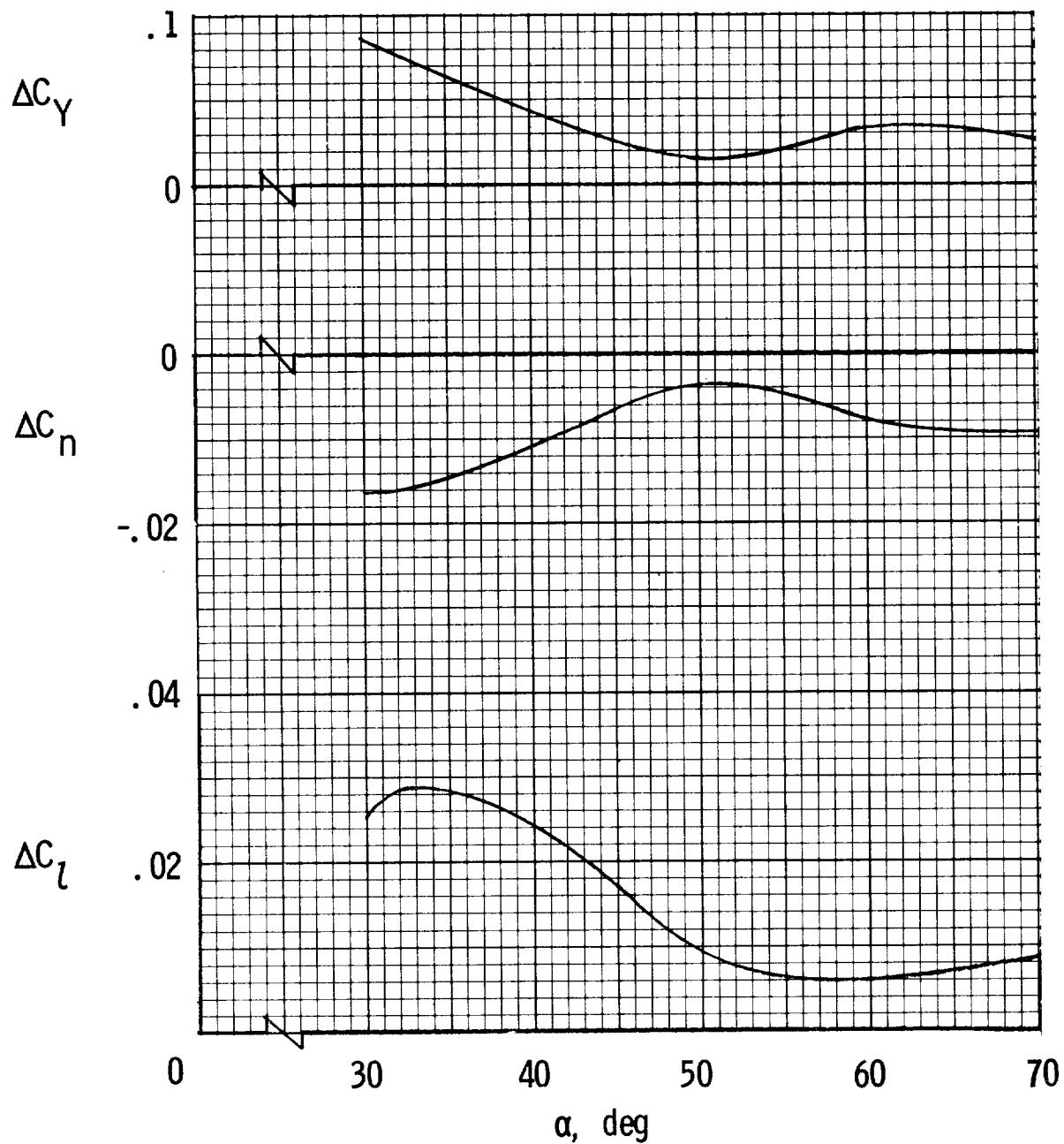
Figure 14.- Average incremental lateral force and moment coefficients produced by differential wing-tip deflection. $\beta = 0^\circ$; $\frac{\Delta l_{L-6}}{l_k} = 0.022$; $\frac{\Delta l_{R-6}}{l_k} = -0.022$.